SPICE Implementation of Multiconductor Transmission Line Model of Transformer Winding for Very Fast Transient Analysis

Amir Ali Kaabi Nejadian, Hamed Moradi Tavasani, Manuja Gunawardana, Waldemar Ziomek, Behzad Kordi

***Abstract*—To analyze fast transient phenomena in power transformers winding, a distributed, white-box model is developed in this paper. Time domain multiconductor transmission line (MTL) theory is employed. The model is constructed by decoupling the MTL equations using SPICE. The developed time-domain SPICE model, unlike frequency-domain techniques, has the ability to incorporate nonlinear components. Different transformer winding configurations are considered, such as interleaved and continuous disk. The model is validated by comparing to published frequency-domain analysis results.**

***Keywords*—Power transformer; transformer winding; transient simulation; multiconductor transmission line; SPICE.**

I. Introduction

POWER transformers are integral elements of the power system infrastructure. Their efficiency and reliability significantly influence the overall performance of electric power systems. Transformer failures can lead to disruptions in supplying power and significant financial losses [1]. Most of the failures in power transformers stem from fast and very fast transient phenomena such as lightning, internal resonance, and partial discharges (PD) [2].

To analyze the effects of transients on power transformers, three models have been proposed for the simulation of transformer winding. The models can be classified into white-box, black-box, and gray-box models. In black-box modelling, transformer winding is represented based on the frequency response measured at its terminals. [3]. The prime disadvantage of black-box modelling is its lack of providing a physical insight of the transformer, making them not preferred for internal fault analysis and resonance. Unlike the black-box models, the white-box models uses detailed physical and electrical characteristics of the transformer winding to reproduce its transient behavior [4]. This method requires geometrical data, allowing for an accurate description of the internal voltage distribution. The purpose of using gray box modeling is to build a physical model of the transformer winding based on the frequency response measurement without having any information on the geometrical and construction information [5].

For an accurate analysis of the transformer response to fast and very fast transient phenomena, white-box modelling should be used [4]. Two approaches have been developed for the implementation of a transformer's white-box model: the lumped-element model and the distributed-parameter models [6]. Lumped-element models are suitable for practical computations because they are simple and easy to implement [7], [8]. However, the distributed parameter model of power transformers, which can be represented as multiconductor transmission lines (MTL), are more accurate for very fast transient phenomena [9]. The distributed-parameter model can be represented in both the frequency-domain and the time-domain. In the frequency-domain analysis, fast transient are analyzed using fast Fourier Transform (FFT) and inverse fast Fourier Transform (IFFT), and superposition principle [10], [11]. This approach has several advantages such as incorporating frequency-dependent losses and fast simulation, but it is only valid for linear systems and devices and requires the repetition of the analysis at many frequencies points. Time-domain analysis on the other hand can handle nonlinear systems and only execution of the simulation/analysis is needed.

In this paper, a SPICE-based transformer winding model in the time domain is developed that employs MTL representation of winding conductors. (SPICE is a commonly used software tool for simulating and analyzing linear/nonlinear electric and electronic circuits.) Dependent voltage and current sources are used to implement phase-to-mode and mode-to-phase transformations. This allows us to use the built-in SPICE model of a lossless, single-conductor transmission line for simulating an MTL structure. This approach offers several advantages, including detailed insight into the transient behavior of transformer winding and providing a better understanding of voltage and current distributions during fault conditions. This methodology facilitates the incorporation of transformer windings in a time-domain SPICE environment, enabling the analysis of nonlinear elements. In the following, an overview of the proposed methodology and examples are presented to verify its accuracy.

This work was supported in part by Natural Sciences and Engineering Research Council of Canada (NSERC) and Mitacs. A. A. Kaabi Nejadian and B. Kordi are with the University of Manitoba, Winnipeg, MB, Canada (e-mail of corresponding author: behzad.kordi@umanitoba.ca). H. Moradi Tavasani is with Electric Power Engineers, Austin, TX, USA. M. Gunawardana is with the University of Moratuwa, Sri Lanka. W. Ziomek is with PTI Transformers and the University of Manitoba, Winnipeg, MB, Canada.

Paper submitted to the International Conference on Power Systems Transients (IPST2025) in Guadalajara, Mexico, June 8-12, 2025.

II. Multiconductor Transmission Line Model of Power Transformers in Time-Domain

The conductors of a typical power transformer winding are arranged in multiple disks, with each disk consisting of multiple turns. Unlike 50/60 Hz voltages and currents that follow the transformer winding conductors as their electrical path, the flow path of fast and very fast transients is determined by their frequency content. Higher frequency components travel through both the conductors and stray/parasitic capacitances that exist between the turns ad between the disks.

The travel time of fast transients in large power transformers becomes comparable to the risetime of the transient. Alternatively, in the frequency domain, the size of the winding becomes comparable to the smallest wavelength of the transient signal. As such, multiconductor transmission line (MTL) theory should be utilized for more accurate determination of the propagation of transients. In this approach, each turn of either LV or HV windings is modeled as a conductor of an MTL structure. In other words, the developed MTL structure can include both the LV and HV windings and any mutual coupling between them. The MTL model is shown in Fig. 1.

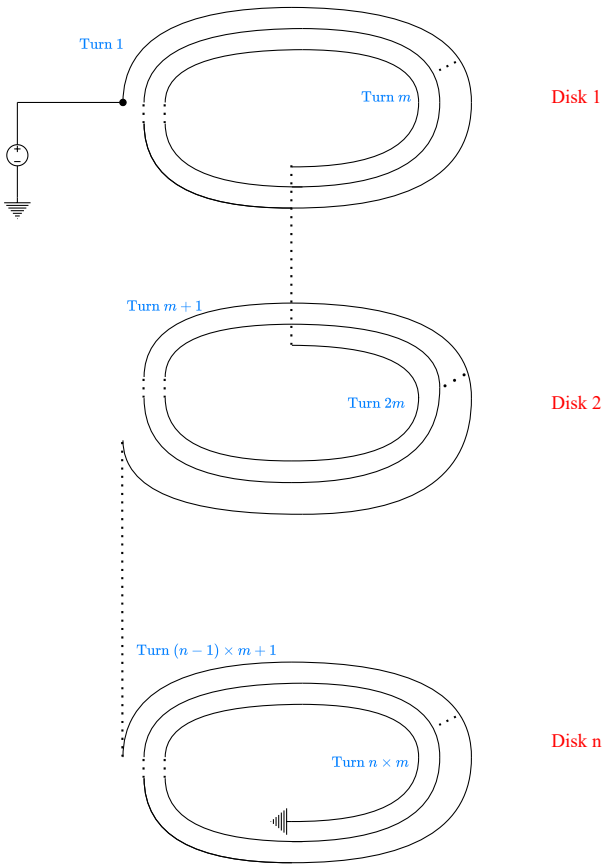

Fig. 1. Schematic of MTL modeling of a continuous-disk transformer winding consisting of n disks with m turns per disk.

Neglecting the curvature of conductors in the model shown in Fig. 1, the voltage and current of every conductor in a lossless MTL can be determined by solving [12]

$$\begin{aligned}\frac{\partial \mathbf{V}(z,t)}{\partial z} &= -\mathbf{L}\frac{\partial \mathbf{I}(z,t)}{\partial t}\\ \frac{\partial \mathbf{I}(z,t)}{\partial z} &= -\mathbf{C}\frac{\partial \mathbf{V}(z,t)}{\partial t}\end{aligned} \tag{1}$$

where $\mathbf{V}(z,t)$ and $\mathbf{I}(z,t)$ are vectors of conductors voltage and current at position z and time t, respectively, and $\mathbf{L}$ and $\mathbf{C}$ are the per unit length (PUL) inductance and capacitance matrices of the MTL. To enable time domain simulation of the MTL equations, the medium and the conductors are considered to be lossless [13]. The impact of neglecting loss on the simulation results is discussed later.

A. Decoupling of MTL Equations

For the case of an MTL with of $n+1$ conductors (i.e. n conductors plus 1 reference conductor), (1) consists of $2n$ coupled partial differential equations. Below is a brief overview of using similarity transformation for decoupling (1) [12].

Similarity transformation matrices $\mathbf{T}_V$ and $\mathbf{T}_I$ are defined by

$$\begin{aligned}\mathbf{V}(z,t) &= \mathbf{T}_V\mathbf{V}_m(z,t)\\ \mathbf{I}(z,t) &= \mathbf{T}_I\mathbf{I}_m(z,t)\end{aligned} \tag{2}$$

to transform the vectors of mode voltage $\mathbf{V}_m(z,t)$ and current $\mathbf{I}_m(z,t)$ to the vectors of actual (phase) voltage $\mathbf{V}(z,t)$ and current $\mathbf{I}(z,t)$. Substituting (2) into (1) yields

$$\begin{aligned}\frac{\partial}{\partial z}\mathbf{V}_m(z,t) &= -\mathbf{T}_V^{-1}\mathbf{L}\mathbf{T}_I\frac{\partial}{\partial t}\mathbf{I}_m(z,t)\\ \frac{\partial}{\partial z}\mathbf{I}_m(z,t) &= -\mathbf{T}_I^{-1}\mathbf{C}\mathbf{T}_V\frac{\partial}{\partial t}\mathbf{V}_m(z,t)\end{aligned} \tag{3}$$

Matrices $\mathbf{T}_V$ and $\mathbf{T}_I$ are determined such that the $2n$ equations of (3) become decoupled. Defining

$$\begin{aligned}\mathbf{L}_m &= \mathbf{T}_V^{-1}\mathbf{L}\mathbf{T}_I\\ \mathbf{C}_m &= \mathbf{T}_I^{-1}\mathbf{C}\mathbf{T}_V\end{aligned} \tag{4}$$

the $2n$ equations of (3) are decoupled if matrices $\mathbf{L}_m$ and $\mathbf{C}_m$ are diagonal,

$$\mathbf{L}_m = \begin{bmatrix} l_{\mathrm{m1}} & 0 & \cdots & 0\\ 0 & l_{\mathrm{m2}} & \ddots & \vdots\\ \vdots & \ddots & \ddots & 0\\ 0 & \cdots & 0 & l_{\mathrm{mn}}\end{bmatrix}$$
$$\mathbf{C}_m = \begin{bmatrix} c_{\mathrm{m1}} & 0 & \cdots & 0\\ 0 & c_{\mathrm{m2}} & \ddots & \vdots\\ \vdots & \ddots & \ddots & 0\\ 0 & \cdots & 0 & c_{\mathrm{mn}}\end{bmatrix}. \tag{5}$$

Selecting $\mathbf{T}_V$ and $\mathbf{T}_I$ as [12]

$$\begin{aligned}\mathbf{T}_V &= \mathscr{E}\{\mathbf{LC}\}\\ \mathbf{T}_I &= \mathscr{E}\{\mathbf{CL}\}\end{aligned} \tag{6}$$

where $\mathscr{E}\{.\}$ is the eigenvector operator, allows us to decouple the $2n$ equations in (1). Once the MTL equations are

decoupled, each mode can be treated as a single conductor transmission line with the characteristic impedance, the propagation speed, and time delay of the i^{th} mode given by

$$Z_{Cmi} = \sqrt{\frac{l_{mi}}{c_{mi}}} \tag{7}$$

$$v_{mi} = \frac{1}{\sqrt{l_{mi} c_{mi}}} \tag{8}$$

$$T_{Dmi} = \frac{\ell}{v_{mi}} \tag{9}$$

where ℓ is the length of the conductor.

III. MTL Model of Winding in SPICE

Figure 2 shows the SPICE model implemented in this paper to solve (1). The model consists of 3 sections. In sections I and III, we have access to the actual (phase) voltages and currents at the two ends of each turn, respectively. Sections II consists of single-conductor transmission lines in the mode domain. As shown in Fig. 2, phase-to-mode and mode-to-phase transformations have been implemented using dependent voltage and current sources given by [12]

$$\begin{aligned} E_i &= \sum_{k=1}^{n} \left[\mathbf{T}_V\right]_{ik} V_{mk}(0,t) \\ F_i &= \sum_{k=1}^{n} \left[\mathbf{T}_I^{-1}\right]_{ik} I_k(0,t) \\ E_i' &= \sum_{k=1}^{n} \left[\mathbf{T}_V\right]_{ik} V_{mk}(L,t) \\ F_i' &= \sum_{k=1}^{n} \left[\mathbf{T}_I^{-1}\right]_{ik} I_k(L,t) \end{aligned} \tag{10}$$

where n is the number of conductors (i.e. number of turns), $\left[\mathbf{T}_V\right]_{ik}$ and $\left[\mathbf{T}_I^{-1}\right]_{ik}$ are the ik^{th} elements of $\mathbf{T}_V$ and inverse of $\mathbf{T}_I$ matrices, respectively.

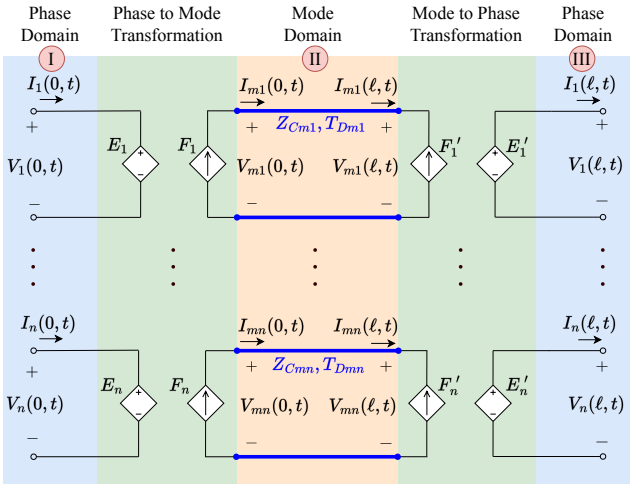

Fig. 2. A SPICE model of an MTL where phase-to-mode and mode-to-phase transformations have been implemented using dependent voltage and current sources.

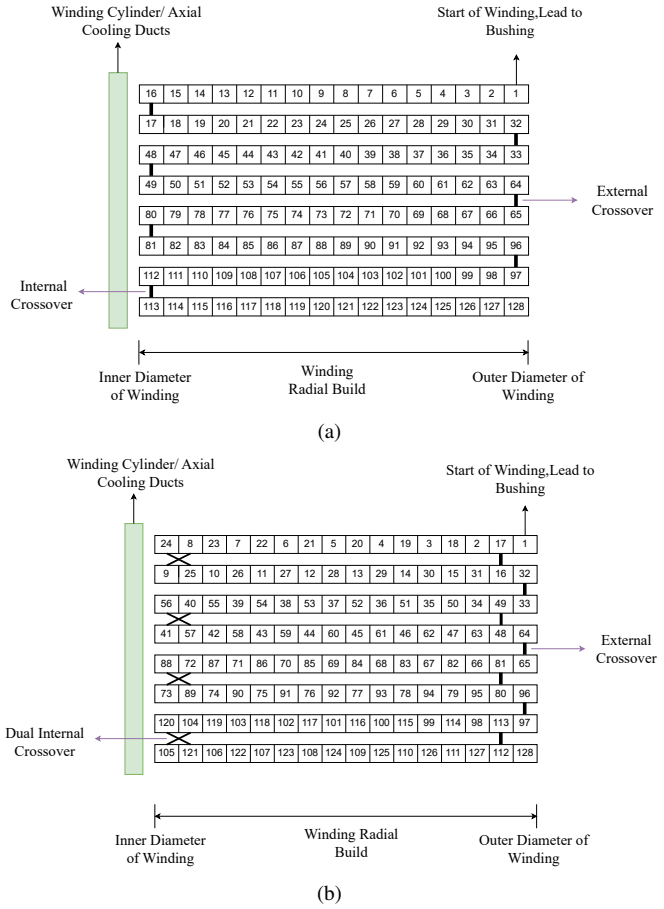

Fig. 3. Cross-sectional view of a) an eight disk continuous-disk winding and b) an eight disk interleaved winding.

A. Winding Configuration

Two most common configurations used in transformer design include continuous-disk and interleaved windings. Figures 3 (a) and (b) show examples of turn connections for these two types of windings. The winding shown in these figures consists of 8 disks with 16 turns in each disk. The SPICE model of this winding consists of an MTL with 128 (i.e. 8×16) conductors.

Interconnection of the MTL conductors in the SPICE model determines the type of the winding. For example, to implement a continuous-disk winding in SPICE, the conductors are connected such that

$$\begin{aligned} V_1(0,t) &= V_S(t) \\ V_i(L,t) &= V_{i+1}(0,t) \quad (i = 1, 2, \cdots, N-1) \\ I_i(L,t) &= I_{i+1}(0,t) \quad (i = 1, 2, \cdots, N-1) \\ V_N(L,t) &= 0. \end{aligned} \tag{11}$$

In this implementation, the turns are continuously connected, the beginning of the widning is connected to the voltage source $V_S(t)$, and the end of the winding is grounded.

IV. Determination of PUL Parameters

To determine the PUL inductance $\mathbf{L}$ and capacitance $\mathbf{C}$ matrices of a given winding, we employ finite element method

(FEM) to solve magnetostatic and electrostatic equations. This assumes that the variation of $\mathbf{L}$ and $\mathbf{C}$ matrices with frequency is negligible [10]. An axisymmetric model is used to include the winding turns curvature. The tank and the core are considered as perfect electrical conductors (PEC), which is a reasonable assumption at high frequencies [14]. The advantage of using FEM approach is the calculation of the PUL parameters of a winding with an arbitrary geometrical cross section.

A. Calculation of Inductance and Capacitance Matrices

To calculate the capacitance matrix $\mathbf{C}$, the electrostatic problem described by

$$\nabla^2 V(r,z) = 0 \tag{12}$$

is solved. In (12), V is the electric potential and ∇^2 represents the Laplacian operator. The elements of $\mathbf{C}$ are calculated using

$$C_{ij} = \left.\frac{q_i}{V_j}\right|_{V_1=\cdots=V_{j-1}=V_{j+1}=\cdots=V_n=0} \tag{13}$$

where V_j is a known voltage (e.g. 1 V) applied to the j^{th} conductor and q_i is the charge of conductor i.

To calculate the inductance matrix $\mathbf{L}$, the magnetostatic problem described by

$$\nabla^2 A_\varphi(r,z) = 0 \tag{14}$$

is solved to determine the magnetic potential A_φ, where ∇^2 represents the Laplacian operator [10]. By choosing a value of $A_\varphi = 1$ for the i^{th} turn and 0 for the rest of the turns as the boundary conditions, the magnetic flux of the i^{th} turn ψ_i will be equal to 1. The inverse of the inductance is given by

$$L_{ij}^{-1} = \left.\frac{I_i}{\psi_j}\right|_{\psi_1=\cdots=\psi_{j-1}=\psi_{j+1}=\cdots=\psi_n=0} \tag{15}$$

In (15), ψ_j is the magnetic flux between the ground and the conductor j and I_i is the current of conductor i.

B. Incorporation of Loss

The main source of loss in the propagation of fast transients in a transformer winding is the ohmic resistance of the conductors. The frequency-dependent resistance of winding conductors can be calculated using [15]

$$R_{\text{cond}} = \text{Re}\left\{\sqrt{R_{\text{dc}}^2 + Z_{\text{hf}}^2}\right\} \tag{16}$$

where

$$R_{\text{dc}} = \frac{1}{\sigma S}$$

$$Z_{\text{hf}} = \frac{1}{2\sigma(w+h)}\sqrt{j\omega\mu_c\sigma}.$$

In (16), σ, μ_c, S, w, and h are the conductivity of the conductors,the permeability of the conductors, the cross sectional area of the conductors, the width, and the height of conductors cross section, respectively.

Since the built-in single conductor transmission line model in SPICE does not include the distributed resistance of the conductors, a pseudo-lumped model [16] was employed in this work. The pseudo-lumped model is a relatively accurate incorporation of distributed resistance in a transmission line by including two lumped resistors, each equal to the half of the resistance, at each terminal of the lossless transmission line. In this paper, the resistance value at the center of the frequency range (i.e. $\approx$ 3 MHz) is used. The conductance matrix has been neglected in this work, as the value of conductance is so low that it does not have any impact on the simulation results.

V. Results and Discussion

The details of the transformer winding, the core, and the tank used for the time-domain analysis is given in Table I [17]. This example that includes a HV winding only is used to compare the results of this work with those available in the literature [10]. A 3D view of the winding, the core, and the tank is shown in Fig. 4.

TABLE I
GEOMETRICAL DETAILS OF THE WINDING USED IN THIS WORK ADOPTED FROM [17].

Number of turns	128
Number of disks	8
Bare conductor dimensions	12.5×2 mm
Total paper insulation	1 mm
Inside diameter	700 mm
Outside diameter	798 mm
Relative permittivity of paper insulation	3.8
Relative permittivity of transformer oil	2.2
Distance between disks	6 mm
Tank diameter	85 cm
Tank height	22 cm

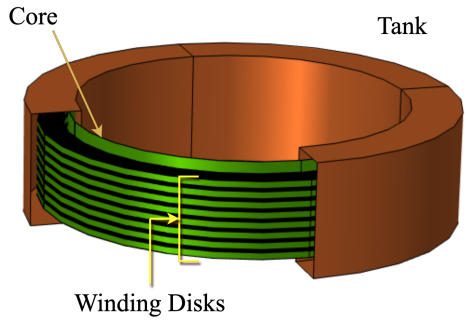

Fig. 4. 3D view of the winding, the core, and the tank given in Table I simulated in this paper and compared with the results available in the literature.

Using this information FEM simulations were performed to calculate the PUL inductance and capacitance matrices. Figure 5 shows the potential distribution results calculated by solving (12) using a commercial FEM software, Comsol Multiphysics. In this figure, the potential of one of the turns is set to 1 V while the other conductors are at ground potential. Using these results, one element of the capacitance matrix is calculated using (13). This procedure is repeated to calculate all the elements of the capacitance matrix $\mathbf{C}$. Similarly the magnetostatic problem given by (14) is solved to determine the inductance matrix $\mathbf{L}$.

The model shown in Fig. 2 that consists of 768 dependent sources was implemented using LTspice[1]. The terminals of

[1]LTspice is a free version of SPICE by Analog Devices.

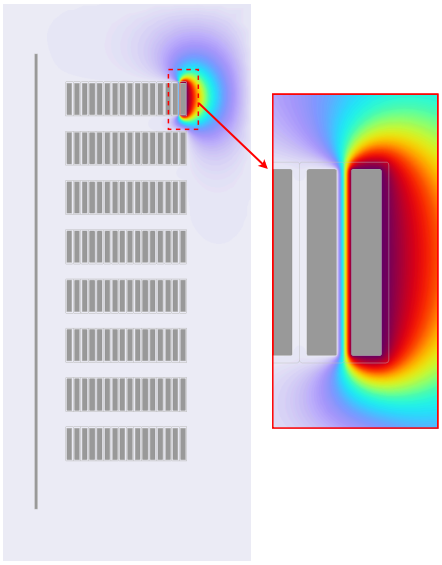

Fig. 5. Potential distribution calculated using FEM when all conductors but one are at ground potential.

the conductors can connected to represent either of the continuous-disk or interleaved windings shown in Fig. 3. To verify the accuracy of the SPICE model, the input admittance of the interleaved and continuous-disk windings has been compared with that obtained using a frequency-domain analysis [10] (see Fig. 6). The SPICE model has been able to accurately determine the resonant frequencies of both types of the winding.

Figure 7 shows the time-domain response of the winding at one of the turns (e.g. turn #15) when a Gaussian voltage waveform is applied as the input to turn 1 (i.e. $V_1(0)$. Two Gaussian waveforms, one with a slow rise time of $5\,\mu$s and the other with a fast rise time of $1\,\mu$s, have been used. This figure shows that the fast rise time pulse has excited internal resonances. Internal resonances are known to generate inter-turn voltages that exceed the insulation withstand and cause failures [18].

To determine the voltage distribution along the winding, a $1\,\mu$s Gaussian voltage is applied to the first turn and the peak of the voltage is determined at every turn. The variation of the peak voltage along the winding is shown in Fig. 8. As expected the voltage distribution is more linear for the interleaved winding [19].

VI. Conclusions

In this paper, a time-domain MTL model for the transient analysis of a transformer winding using SPICE is presented. This approach involves decoupling the MTL equations using dependent voltage and current sources and the lossless transmission line model of SPICE. A pseudo-lumped was used to incorporate the loss in the model. One of the main advantages of this method is its ability to provide rapid simulations in time-domain analysis. Unlike frequency domain models, nonlinear and time-varying components can be directly be added to this model, making it versatile for a wide range of applications. A comparison between

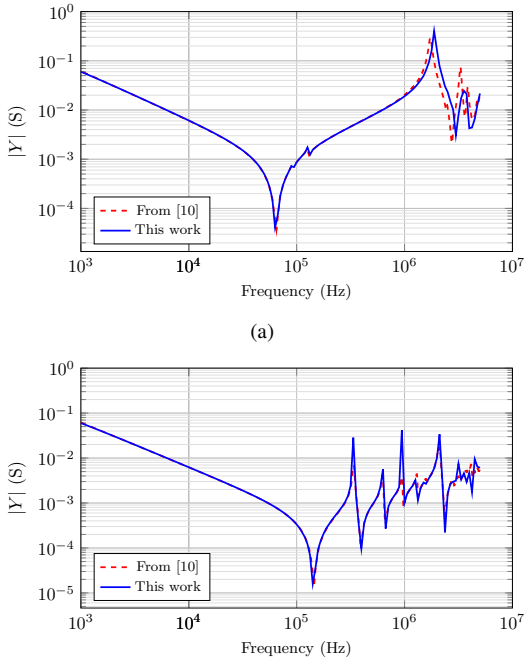

Fig. 6. Comparison of the magnitude of the winding input admittance calculated using the SPICE model developed in this work and the frequency domain analysis [10] for a) interleaved and b) continuous-disk configurations.

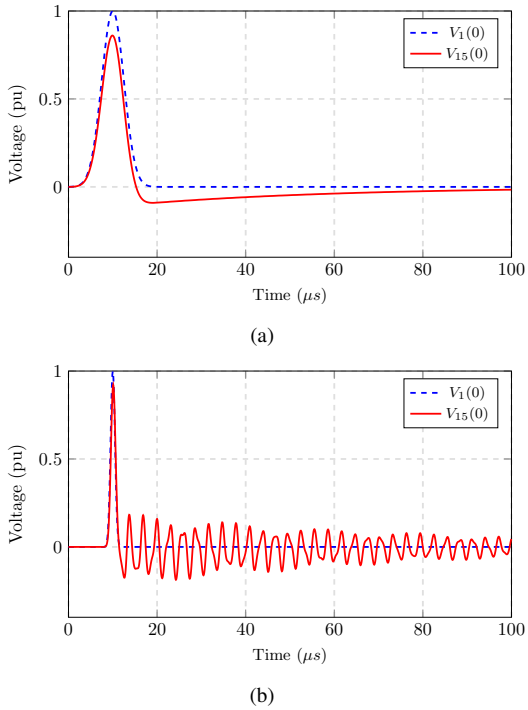

Fig. 7. Voltage of the 15^{th} turn when a Gaussian waveform with a) a slow rise time ($5\,\mu$s) and b) a fast rise time ($1\,\mu$s) is applied as the input at turn 1 of the continuous-disk winding. The high frequency content of the fast Gaussian pulse excites the internal resonance of the winding.

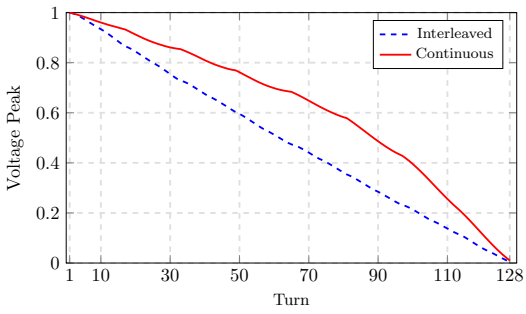

Fig. 8. Voltage distribution across transformer winding in both continuous and interleaved disk configurations.

frequency-domain and time-domain analyses demonstrates that the proposed time-domain technique offers high accuracy.

REFERENCES

[1] A. R. Abbasi, "Fault detection and diagnosis in power transformers: a comprehensive review and classification of publications and methods," *Electric Power Systems Research*, vol. 209, p. 107990, 2022.

[2] M. R. Hussain, S. S. Refaat, and H. Abu-Rub, "Overview and partial discharge analysis of power transformers: A literature review," *IEEE Access*, vol. 9, pp. 64 587–64 605, 2021.

[3] D. Filipović-Grčić, B. Filipović-Grčić, and I. Uglešić, "High-frequency model of the power transformer based on frequency-response measurements," *IEEE Trans. Power Delivery*, vol. 30, pp. 34–42, 2015.

[4] E. E. Mombello, "New compact white-box transformer model for the calculation of electromagnetic transients," *IEEE Trans. Power Delivery*, vol. 37, no. 4, pp. 2921–2931, 2022.

[5] R. Aghmasheh, V. Rashtchi, and E. Rahimpour, "Gray box modeling of power transformer windings based on design geometry and particle swarm optimization algorithm," *IEEE Transactions on Power Delivery*, vol. 33, no. 5, pp. 2384–2393, 2018.

[6] W. Song, Z. Wang, S. Tian, J. Guo, Y. Chen, and Y. Xie, "Simulation of short circuit to ground of transformer winding based on mtl model," in *2022 4th International Conference on Power and Energy Technology (ICPET)*, 2022, pp. 305–310.

[7] Z. Luna López, P. Gómez, F. P. Espino-Cortés, and R. Peña-Rivero, "Modeling of transformer windings for fast transient studies: Experimental validation and performance comparison," *IEEE Trans. Power Delivery*, vol. 32, no. 4, pp. 1852–1860, 2017.

[8] T. Župan, B. Trkulja, R. Obrist, T. Franz, B. Cranganu-Cretu, and J. Smajic, "Transformer windings' RLC parameters calculation and lightning impulse voltage distribution simulation," *IEEE Trans. Magnetics*, vol. 52, no. 3, pp. 1–4, 2016.

[9] M. Popov, L. van der Sluis, R. P. P. Smeets, and J. Lopez Roldan, "Analysis of very fast transients in layer-type transformer windings," *IEEE Trans. Power Delivery*, vol. 22, no. 1, pp. 238–247, 2007.

[10] M. Gunawardana, F. Fattal, and B. Kordi, "Very fast transient analysis of transformer winding using axial multiconductor transmission line theory and finite element method," *IEEE Trans. Power Delivery*, vol. 34, no. 5, pp. 1948–1956, 2019.

[11] H. Moradi Tavasani, W. Ziomek, K. Kuby, S. Tade, and B. Kordi, "Partial discharge localization in transformer winding using an axial multiconductor transmission line model," in *2023 Cigre Canada Conference and Exhibition*, Vancouver, BC, Canada, 25-28 Sep. 2023.

[12] C. R. Paul, *Analysis of Multiconductor Transmission Lines*, 2nd ed. Wiley-IEEE Press, 2007.

[13] C. Paul, "A simple spice model for coupled transmission lines," in *IEEE 1988 Int. Symp. Electromagnetic Compatibility*, 1988, pp. 327–333.

[14] J. Velasco, "Power system transients: Parameter determination," *Boca Raton, FL, USA: CRC Press*, 2010.

[15] A. Ametani and T. Ohno, "Transmission line theories for the analysis of electromagnetic transients in coil windings," in *Electromagnetic Transients in Transformer and Rotating Machine Windings*, C. Q. Su, Ed. Hershey, PA, USA: IGI Global, Year, ch. 1, pp. 1–45.

[16] C. C. Wong and S. Y. Luk, "Simulation of lossy multi-conductor transmission line systems using spice," in *2001 IEEE Int. Symp. Electromagnetic Compatibility*, vol. 1, 2001, pp. 574–576 vol.1.

[17] M. M. Kane and S. V. Kulkarni, "MTL-based analysis to distinguish high-frequency behavior of interleaved windings in power transformers," *IEEE Trans. Power Delivery*, vol. 28, no. 4, p. 2291–2299, Oct 2013.

[18] M. Babaei and A. Abu-Siada, "Preventing transformer internal resonance under very fast transient overvoltage using RC surge suppressor," *IEEE Transactions on Dielectrics and Electrical Insulation*, vol. 24, no. 2, pp. 1263–1272, 2017.

[19] M. Bagheri, A. Hekmati, R. Heidarzadeh, and M. Salay Naderi, "Impulse voltage distribution in intershield disk winding vs interleaved and continuous disk winding in power transformer," in *2008 IEEE 2nd International Power and Energy Conference*, 2008, pp. 387–392.